molecular pharmaceutics

articles

Coaxial Electrohydrodynamic Spraying: A Novel One-Step Technique To Prepare Oligodeoxynucleotide Encapsulated Lipoplex Nanoparticles

Yun Wu,[†,‡] Bo Yu,[†,‡] Andrew Jackson,[§,||] Weibin Zha,[‡] L. James Lee,[†,‡] and Barbara E. Wyslouzil*[,†,‡,⊥]

William G. Lowrie Department of Chemical and Biomolecular Engineering, The Ohio State University, 140 West 19th Avenue, Columbus, Ohio 43210, NSF Nanoscale Science and Engineering Center, The Ohio State University, 174 West 18th Avenue, Columbus, Ohio 43210, Department of Chemistry, The Ohio State University, 100 West 18th Avenue, Columbus, Ohio 43210, NIST Center for Neutron Research, National Institute of Standards and Technology, Gaithersburg, Maryland 20899, and Department of Materials Science and Engineering, University of Maryland, College Park, Maryland 20742

Received January 27, 2009; Revised Manuscript Received May 19, 2009; Accepted May 21, 2009

Abstract: This study investigates coaxial electrohydrodynamic spraying (electrospray for short) as a novel, rapid, real time and single-step method to produce oligodeoxynucleotide (ODN) encapsulated lipoplex nanoparticles for either intravenous injection or, potentially, pulmonary delivery. Using a coaxial needle setup, we produced G3139 (oblimerson sodium, or Genasense) encapsulated lipoplex nanoparticles, and investigated the effects of production parameters on nanoparticle size and structure. Careful control of production parameters yielded lipoplex nanoparticles 190 ± 39 nm in diameter with unilamellar structure and 90 ± 6% encapsulation efficiency of G3139. Both nontargeted and transferrin-targeted G3139 lipoplex nanoparticles were efficiently delivered to K562 cells and downregulated the bcl-2 protein expression by 34 ± 6% and 57 ± 3% respectively.

Keywords: Coaxial electrospray; oligonucleotide; G3139; lipoplex; nanoparticles

1. Introduction

Lipoplex nanoparticles have phospholipid bilayer structures that can encapsulate aqueous medium. These structures are of great interest in the gene and drug delivery field because they can carry active drugs or genes within the hydrophobic bilayers or in the hydrophilic core. Traditional methods used to prepare lipoplex nanoparticles include bulk mixing,[1,2] the dehydration−rehydration method,[1] the film method (Bangham method),[3,4] freeze−thaw extrusion,[5] the detergent depletion method,[6] ultrasonication,[7] alcohol

* To whom correspondence should be addressed. Mailing address: The Ohio State University, Department of Chemical and Biomolecular Engineering, 140 W 19th Avenue, Columbus, OH 43210. Phone: (614) 688-3583. Fax: (614) 292-3769. E-mail: wyslouzil.1@osu.edu.

† Department of Chemical and Biomolecular Engineering, The Ohio State University.

‡ NSF Nanoscale Science and Engineering Center, The Ohio State University.

§ National Institute of Standards and Technology.

|| University of Maryland.

⊥ Department of Chemistry, The Ohio State University.

(1) Chrai, S. S.; Murari, R.; Ahmad, I. Liposomes (a review) part one: manufacturing issues. *BioPharm* **2001**, *13*, 10–14.

(2) Elouahabi, A.; Ruysschaert, J. Formation and intracellular trafficking of lipoplexes and polyplexes. *Mol. Ther.* **2005**, *11*, 336–347.

(3) Fan, M.; Xu, S.; Xia, S.; Zhang, X. Effect of different preparation methods on physicochemical properties of salidroside liposomes. *J. Agric. Food Chem.* **2007**, *55*, 3089–3095.

(4) Otake, K.; Shimomura, T.; Goto, T.; Imura, T.; Furuya, T.; Yoda, S.; Takebayashi, Y.; Sakai, H.; Abe, M. Preparation of liposomes using an improved supercritical reverse phase evaporation method. *Langmuir* **2006**, *22*, 2543–2550.

(5) Chapman, C. J.; Erdahl, W. E.; Taylor, R. W.; Pfeiffer, D. R. Effects of solute concentration on the entrapment of solutes in phospholipid vesicles prepared by freeze-thaw extrusion. *Chem. Phys. Lipids* **1991**, *60*, 201–208.

10.1021/mp9000348 CCC: $40.75
Published on Web 06/05/2009

dilution,[8−11] and the reverse phase evaporation method.[12] Limitations of the standard technologies include the production of lipoplex nanoparticles with polydisperse size distributions, low encapsulation efficiency of the gene or drug, and complicated multistep preparation processes.[13,14]

Antisense oligodeoxynucleotides (ODN), short pieces of specially designed DNA, can hybridize to specific mRNA sequences, inhibit gene expression by RNase-H activation or steric blocking, and thus interfere in the synthesis of a particular protein and prevent the disease from progressing. ODN has been widely investigated as a potential therapeutic agent against viral infections, cardiovascular inflammation, hematological malignancies, pulmonary diseases and cancer.[9,10] G3139 is an 18-mer ODN (5′-TCT CCC AGC GTG CGC CAT-3′). It is specially designed to bind the first six codons of the human bcl-2 mRNA and thus inhibit the bcl-2 expression, and may provide a way to decrease the resistance of tumor cells to chemotherapy.[9]

The ethanol dilution method[8−11] has become a popular way to prepare ODN containing lipoplex nanoparticles. Briefly, lipids are first dissolved in ethanol and then mixed with the aqueous ODN buffer solution. The mixture is dialyzed against buffer solutions with different pH values to form ODN encapsulated lipoplex nanoparticles. This preparation process involves multiple steps and can take days to complete, and contamination introduced during the dialysis steps can be a problem.

Electrohydrodynamic spraying (electrospray for short), an aerosol technique, uses electrical forces to atomize liquids. A great deal of research has been done to explore the potential applications of electrospray.[15−18] In biological applications, electrospray is well-known for its use in electrospray ionization mass spectrometry (EI-MS).[19] Using single needle electrospray, biological materials, such as alkaline phosphatase,[16] bovine serum albumin (BSA),[20] insulin,[21] DNA,[22,23] and cells,[24] have also been electrosprayed without changing the biological activity of these materials. Xie et al. produced BSA or paclitaxel encapsulated PLGA particles for controlled release applications.[25,26] In 2002, Loscertales et al. first developed a coaxial electrospray setup using concentric needles to produce water/oil capsules with size ranging from 10 μm to 150 nm.[27] Since then coaxial electrosprays have been applied to produce core−shell particles,[28,29] hollow fibers[30] and microbubbles.[31] In the

(6) Lasic, D. D. The mechanism of vesicle formation. *Biochem. J.* **1988**, *256*, 1–11.

(7) Pereira-Lachataignerais, J.; Pons, R.; Panizza, P.; Courbin, L.; Rouch, J.; Lopez, O. Study and formation of vesicle systems with low polydispersity index by ultrasound method. *Chem. Phys. Lipids* **2006**, *140*, 88–97.

(8) Stano, P.; Bufali, S.; Pisano, C.; Bucci, F.; Barbarino, M.; Santaniello, M.; Carminati, P.; Luisi, P. L. Novel camptothecin analogue (gimatecan)-containing liposomes prepared by the ethanol injection method. *J. Liposome Res.* **2004**, *14*, 87–109.

(9) Chiu, S.; Liu, S.; Perrotti, D.; Marcucci, G.; Lee, R. J. Efficient delivery of a Bcl-2-specific antisense oligodeoxyribonucleotide (G3139) via transferrin receptor-targeted liposomes. *J. Controlled Release* **2006**, *112*, 199–207.

(10) Yang, L.; Li, J.; Zhou, W.; Yuan, X.; Li, S. Targeted delivery of antisense oligodeoxynucleotides to folate receptor-overexpressing tumor cells. *J. Controlled Release* **2004**, *95*, 321–331.

(11) Jeffs, L. B.; Palmer, L. R.; Ambegia, E. G.; Giesbrecht, C.; Ewanick, S.; MacLachlan, I. A. Scalable, Extrusion-Free Method for Efficient Liposomal Encapsulation of Plasmid DNA. *Pharm. Res.* **2005**, *22*, 363–372.

(12) Szoka, F.; Papahadjopoulos, D. Procedure for Preparation of Liposomes with Large Internal Aqueous Space and High Capture by Reverse-Phase Evaporation. *Proc. Natl. Acad. Sci. U.S.A.* **1978**, *75*, 4194–4198.

(13) Müller, R. H.; Keck, C. M. Challenges and solutions for the delivery of biotech drugs - a review of drug nanocrystal technology and lipid nanoparticles. *J. Biotechnol.* **2004**, *113*, 151–170.

(14) Müller, R. H.; Mader, K.; Gohla, S. Solid lipid nanoparticles (SLN) for controlled drug delivery - a review of the state of the art. *Eur. J. Pharm. Biopharm.* **2000**, *50*, 161–177.

(15) Cloupeau, M.; Prunet-Foch, B. Electrohydrodynamic spraying functioning modes: a critical review. *J. Aerosol Sci.* **1994**, *25*, 1021–1036.

(16) Salata, O. V. Tools of Nanotechnology: Electrospray. *Curr. Nanosci.* **2005**, *1*, 25–33.

(17) Jaworek, A.; Sobczyk, A. T. Electrospraying route to nanotechnology: An overview. *J. Electrost.* **2008**, *66*, 197–219.

(18) Jaworek, A. Micro- and nanoparticle production by electrospraying. *Powder Technol.* **2007**, *176*, 18–35.

(19) Fenn, J. B.; Mann, M.; Meng, C. K.; Wong, S. F.; Whitehouse, C. M. Electrospray Ionization for Mass Spectrometry of Large Biomolecules. *Science* **1989**, *246*, 64–71.

(20) Pareta, R.; Brindley, A.; Edirisinghe, M. J.; Jayasinghe, S. N.; Lukinska, Z. B. Electrohydrodynamic atomization of protein (bovine serum albumin). *J. Mater. Sci.: Mater. Med.* **2005**, *16*, 919–925.

(21) Gomez, A.; Bingham, D.; De Juan, L.; Tang, K. Production of protein nanoparticles by electrospray drying. *J. Aerosol Sci.* **1998**, *29*, 561–574.

(22) Chen, D. R.; Wendt, C. H.; Pui, D. Y. H. A novel approach for introducing bio-materials into cells. *J. Nanopart. Res.* **2000**, *2*, 133–139.

(23) Davies, L. A.; Hannavy, K.; Davies, N.; Pirrie, A.; Coffee, R. A.; Hyde, S. C.; Gill, D. R. Electrohydrodynamic comminution: a novel technique for the aerosolisation of plasmid DNA. *Pharm. Res.* **2005**, *22*, 1294–1304.

(24) Jayasinghe, S. N.; Qureshi, A. N.; Eagles, P. A. M. Electrohydrodynamic jet processing: an advanced electric-field-driven jetting phenomenon for processing living cells. *Small* **2006**, *2*, 216–219.

(25) Xie, J.; Lim, L. K.; Phua, Y.; Hua, J.; Wang, C. Electrohydrodynamic atomization for biodegradable polymeric particle production. *J. Colloid Interface Sci.* **2006**, *302*, 103–112.

(26) Xie, J.; Wang, C. Encapsulation of Proteins in Biodegradable Polymeric Microparticles Using Electrospray in the Taylor Cone-Jet Mode. *Biotechnol. Bioeng.* **2007**, *97*, 1278–1290.

(27) Loscertales, I. G.; Barrero, A.; Guerrero, I.; Cortijo, R.; Marquez, M.; Ganan-Calvo, A. M. Micro/Nano encapsulation via electrified coaxial liquid jets. *Science* **2002**, *295*, 1695–1698.

(28) Hwang, Y. K.; Jeong, U.; Cho, E. C. Production of uniform-sized polymer core-shell microcapsules by coaxial electrospraying. *Langmuir* **2008**, *24*, 2446–2451.

(29) Larsen, G.; Velarde-Ortiz, R.; Minchow, K.; Barrero, A.; Loscertales, I. G. A Method for Making Inorganic and Hybrid (Organic/Inorganic) Fibers and Vesicles with Diameters in the Submicrometer and Micrometer Range via Sol-Gel Chemistry and Electrically Forced Liquid Jets. *J. Am. Chem. Soc.* **2003**, *125*, 1154–1155.

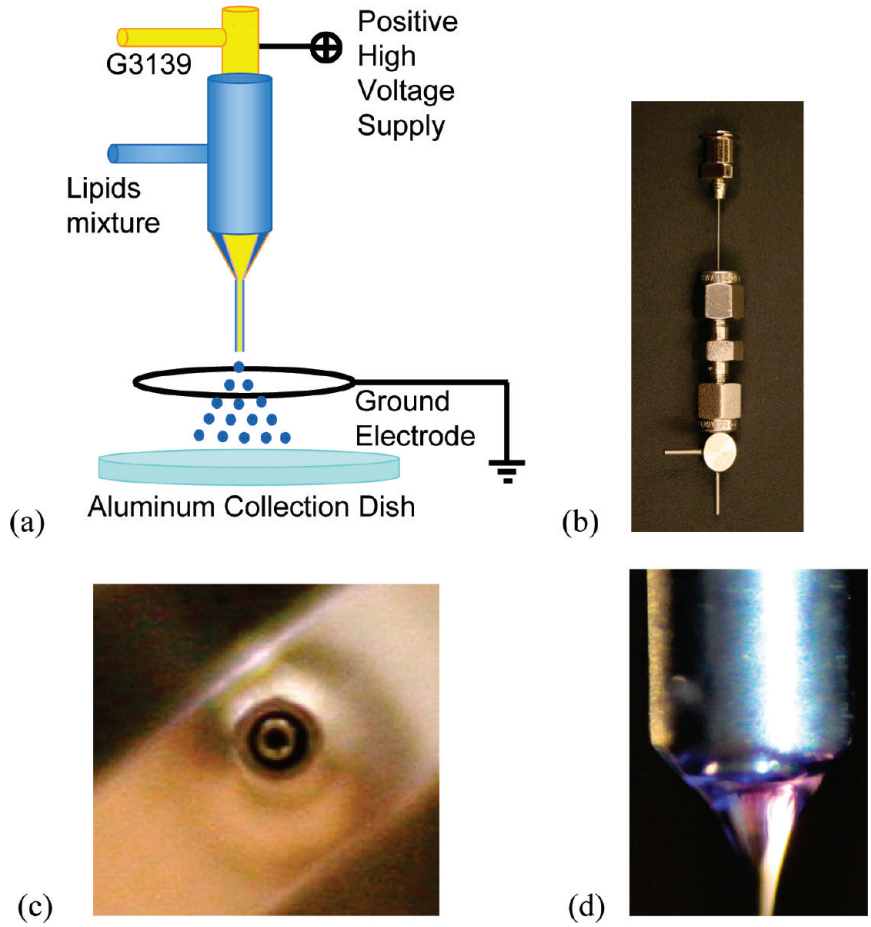

Figure 1. (a) A schematic diagram of the coaxial electrospray setup: the G3139 solution flows through the inner needle, and the lipid mixture flows through the outer needle. A high voltage (≈3 kV) is applied between the inner needle and the grounded electrode. Lipoplex nanoparticles are collected in 1X PBS solutions 10 cm below the tip of the needle. (b) The coaxial needle setup for a 27G inner needle and a 20G outer needle. (c) The tip of the coaxial needles. (d) A photograph of G3139, dyed with crystal violet, and lipid mixture being coaxial electrosprayed in the cone−jet mode.

current study, coaxial electrospray was used to produce G3139 (Genasense or oblimerson sodium) encapsulated lipoplex nanoparticles for either intravenous injection or, potentially, pulmonary delivery. The size and structure of electrosprayed lipoplex nanoparticles was investigated using dynamic light scattering, cryo-transmission electron microscopy (cryo-TEM) and small angle neutron scattering (SANS). The cellular uptake and antisense activity against bcl-2 were evaluated in K562 leukemia cells.

2. Experimental Section

2.1. Materials. Egg phosphatidylcholine (Egg PC) and methoxy-polyethylene glycol (MW ≈2,000 Da)-distearoyl phosphatidylethanolamine (PEG-DSPE) were obtained from Lipoid (Newark, NJ).[32] 3β-[*N*-(*N*′,*N*′-Dimethylaminoethane)-carbamoyl] cholesterol (DC-Chol) and DSPE-PEG-maleimide (DSPE-PEG-Mal) were purchased from Avanti Polar Lipids, Inc. (Alabaster, AL). 2-Iminothiolane (Traut's reagent) and other chemicals were purchased from Sigma Chemical Co. (St. Louis, MO). The phosphorothioate ODN (G3139, 5′-TCT CCC AGC GTG CGC CAT-3′) and the fluorescein modified ODN (FAM-ODN, 5′-(6) FAM-TAC CGC GTG CGA CCC TCT-3′) were custom synthesized by Alpha DNA, Inc. (Montreal, Canada). 200 proof ethanol was purchased from Pharmco-Aaper (E200GP). 1X PBS was purchased from Gibco (14190-136).

2.2. Preparation of G3139 Encapsulated Lipoplex Nanoparticles via Coaxial Electrospray. The G3139 was dispersed in 1X PBS solution. DC-Chol, Egg PC and DSPE-PEG-Mal were dissolved in ethanol at a molar ratio of 30:68:2. As illustrated in Figure 1, the G3139 solution was fed through the inner 27 gauge needle and the lipid mixture was fed through

(30) Loscertales, I. G.; Barrero, A.; Marquez, M.; Spretz, R.; Velarde-Ortiz, R.; Larsen, G. Electrically Forced Coaxial Nanojets for One-Step Hollow Nanofiber Design. *J. Am. Chem. Soc.* **2004**, *126*, 5376–5377.

(31) Farook, U.; Zhang, H. B.; Edirisinghe, M. J.; Stride, E.; Saffari, N. Preparation of microbubble suspensions by co-axial electrohydrodynamic atomization. *Med. Eng. Phys.* **2007**, *29*, 749–754.

(32) The identification of commercial equipment, instruments, materials or suppliers does not imply recommendation or endorsement by the National Institute of Standards and Technology, nor does it imply that the materials or equipment identified are necessarily the best available for the purpose.

the outer 20 gauge needle. A positive voltage, typically ≈3 kV, was applied between the inner needle and a grounded copper ring electrode. As the fluids pass through the needles, the electric field induces free charges at the surface of the liquids. When the electrical stress overcomes the surface tension, the liquid meniscus at the needle opening develops a conical shape, the Taylor cone, followed by a liquid jet. The jet is not stable and, due to varicose or kink instabilities,[15] breaks into an aerosol composed of fine, monodisperse droplets. Ethanol evaporates quickly when the droplets are falling toward the collection dish and the lipoplex nanoparticles are formed. The lipoplex nanoparticles were captured in a grounded aluminum dish 10 cm below the needle tip containing 15 mL of PBS solution. Readers interested in the physics of electrospray are referred to the special issue of *Journal of Aerosol Science* (1999, Volume 30, Issue 7) where detailed theoretical work was presented by Cannan-Calvo et al., Borra et al., Jaworek et al. and many others. For physics of coaxial electrospray, the readers are referred to the work by Loscertales et al.,[27] Lopez-Herreraa et al.,[33] Chen et al.[34] and Mei et al.[35]

2.3. Particle Size and Zeta Potential Measurement. The size distribution of the lipoplex nanoparticles was measured using a NICOMP particle sizer model 370 (Particle Sizing Systems, Santa Barbara, CA). All samples were measured 3 times at room temperature. The zeta potential of the lipoplex nanoparticles was determined by ZetaPALS (Brookhaven Instruments Corp., Worcestershire, NY). All samples were diluted 10-fold with DI water and then measured 5 times at room temperature.

2.4. Small-Angle Neutron Scattering. For small-angle neutron scattering (SANS) measurement, G3139 encapsulated lipoplex nanoparticles were prepared using D_2O instead of H_2O in order to improve contrast, i.e. G3139 was dispersed in 1X PBS/D_2O solution and the electrosprayed lipoplex nanoparticles were collected in 1X PBS/D_2O solution. In addition, the ethanol dilution method was used to prepare G3139 encapsulated lipoplex nanoparticles, which were set as the control. Briefly, the G3139 was dispersed in 1X PBS/D_2O solution and added to the lipid mixture. The final mixture was sonicated slightly in a water bath, followed by two dialysis procedures against citric acid/D_2O (pH = 4.0) and 1X PBS/D_2O (pH = 7.4), respectively.

SANS measurements were performed using the NG7 instrument at the NIST center for Neutron Research in Gaithersburg, MD.[36] The mean incident neutron wavelength was 0.6 nm with a wavelength spread ($\Delta\lambda/\lambda$) of 15%. The samples were loaded in quartz cells with a 4 mm path length and placed in the neutron beam. Data were recorded at sample-to-detector distances of 1.9 m for 3 min and 6 m for 15 min at room temperature. Blocked beam and empty cell scattering data were also recorded under same conditions and used in the SANS data reduction[37] to get the SANS spectrum of the samples.

2.5. Cryo-Transmission Electron Microscopy (Cryo-TEM). One drop of lipoplex nanoparticle sample solution prepared via coaxial electrospray or ethanol dilution was loaded using a micropipet on a lacey Formvar/carbon film coated Cu TEM grid. The excess fluid on the grid surface was removed by blotting the surface with a filter paper. The grid was then plunged into a small vessel of liquid ethane that was located in a larger liquid nitrogen vessel, to vitrify the water film on the grid and to avoid water crystallization. The quenched sample grid was transferred into the grid box that was also stored in liquid nitrogen. The grid was transferred into a Gatan cryo-transfer system filled with liquid nitrogen and loaded onto a cryo-TEM stage. The cryo stage was loaded into the TEM (FEI Tecnai G2 Spirit BioTWIN) and the images were taken at temperatures below −170 °C. The digital images were recorded using a Gatan CCD camera.

2.6. G3139 Encapsulation Efficiency of Coaxial Electrosprayed Lipoplex Nanoparticles. G3139 encapsulation efficiency of coaxial electrosprayed lipoplex nanoparticles was measured semiquantitatively using gel electrophoresis.[38] 1% Triton X-100 was used to break the lipid bilayers and release the encapsulated G3139. Free G3139, the original G3139 encapsulated lipoplex nanoparticles and the G3139 encapsulated lipoplex nanoparticles treated with 1% Triton X-100 were loaded onto a 3% agarose gel containing ethidium bromide (BioRad Laboratories 161-3022). Electrophoresis was carried out at 100 V for 45 min in a 1X TAE running buffer (Invitrogen 15558-026). A digital image of the gel was captured under UV light using a ChemiDoc XRS system (BioRad Laboratories). The density of the bands was measured using ImageJ 1.41o. The G3139 encapsulation efficiency was calculated by comparing the amount of released G3139 with the amount of G3139 used to prepare the lipoplex nanoparticles.

2.7. Cell Culture. K562 cells, obtained from the American type Culture Collection (ATCC) (Manassas, VA), were routinely cultured in a 75 cm^2 T flask containing 15 mL of RPMI 1640 media supplemented with 10% heat-inactivated fetal bovine serum (FBS, Hyclone Laboratories, Logan, UT), 2 mmol/L L-glutamine (Invitrogen, Carlsbad, CA), and penicillin (100 U/mL)/streptomycin (100 μg/mL; Sigma-Aldrich, St. Louis). The cells were seeded into T flasks at a concentration of 3×10^5 viable cells/mL and incubated at 37 °C in a humidified atmosphere containing 5% CO_2.

(33) Lopez-Herreraa, J. M.; Barreroa, A.; Lopezc, A.; Loscertales, I. G.; Marquez, M. Coaxial jets generated from electrified Taylor cones. Scaling laws. *J. Aerosol Sci.* **2003**, *34*, 535–552.

(34) Chen, X.; Jia, L.; Yin, X.; Cheng, J.; Lu, J. Spraying modes in coaxial jet electrospray with outer driving liquid. *Phys. Fluids* **2005**, *17*, 032101.

(35) Mei, F.; Chen, D. Investigation of compound jet electrospray: Particle encapsulation. *Phys. Fluids* **2007**, *19*, 103303.

(36) Glinka, C. J.; Barker, J. G.; Hammouda, B.; Krueger, S.; Moyer, J. J.; Orts, W. J. The 30 m Small-Angle Neutron Scattering Instruments at the National Institute of Standards and Technology. *J. Appl. Crystallogr.* **1998**, *31*, 430–445.

(37) Kline, S. R. Reduction and Analysis of SANS and USANS Data using Igor Pro. *J. Appl. Crystallogr.* **2006**, *39*, 895–900.

(38) Mathew, E.; Hardee, G. E.; Bennett, C. F.; Lee, K.-D. Cytosolic delivery of antisense oligonucleotides by listeriolysin O-containing liposomes. *Gene Ther.* **2003**, *10*, 1105–1115.

2.8. Transfection Studies of G3139 Encapsulated Lipoplex Nanoparticles. Both nontargeted G3139 encapsulated lipoplex nanoparticles and transferrin (Tf)-targeted G3139 encapsulated lipoplex nanoparticles were used to investigate the transfection efficiency. Tf-targeted G3139 encapsulated lipoplex nanoparticles were prepared as described previously.[12] Briefly, Holo-Tf (diferric Tf) was reacted with 5X Traut's reagent to form holo-Tf-SH. The holo-Tf-SH was then reacted with micelles of DSPE-PEG-Mal to yield Tf-PEG-DSPE micelles. The Tf-PEG-DSPE micelles were incubated with lipoplex nanoparticles for 1 h at 37 °C to form Tf-targeted lipoplex nanoparticles.

K562 cells were seeded in 25 cm^2 T-flasks containing 5 mL of cell culture medium at 5×10^5 viable cells/mL. The cells were incubated at 37 °C in a humidified atmosphere containing 5% CO_2 for 2 h. Free G3139, nontargeted G3139 encapsulated lipoplex nanoparticles and Tf-targeted G3139 encapsulated lipoplex nanoparticles were then added into the medium. The cells were incubated at 37 °C for another 4 h, and the transfection process was stopped by transferring cells into 5 mL of fresh medium. Cells were incubated in fresh medium for 48 h and then harvested for the analyses.

2.9. Quantification of Bcl-2 Protein Expression in K562 Cells by Western Blot. 48 h after the transfection process, the cells were washed with 1X PBS twice and then incubated with a lysis buffer containing a protease inhibitor cocktail (CalBiochem, San Diego, CA) on ice for 15 min. The cell lysate was centrifuged for 15 min at 10000*g* at 4 °C. The protein concentration of the supernatant was measured by bicinchoninic acid (BCA) assay (Pierce, Rockford, IL), and 50 μg of protein from each sample was loaded in a 15% Ready Gel Tris-HCl polyacrylamide gel (BioRed, Hercules, CA), and then transferred to a PVDF membrane. After blocking with 5% mass fraction nonfat milk in Tris-buffered saline/Tween-20 for 2 h, the membranes were incubated with monoclonal mouse antihuman bcl-2 or monoclonal mouse antihuman tubulin (Santa Cruz Biotechnology, Santa Cruz, CA) at 4 °C overnight, followed by incubation with horseradish peroxidase-conjugated goat antimouse IgG (Santa Cruz Biotechnology, Santa Cruz, CA) for 1 h at room temperature. The membrane was then developed with Pierce SuperSignal West Pico or Dura Extended Duration Substrate (Pierce, Rockford, IL) and imaged with Kodak X-OMAT film (Kodak, Rochester, NY).

2.10. Cellular Uptake of ODN Encapsulated Lipoplex Nanoparticles. The cellular uptake of ODN encapsulated lipoplex nanoparticles was studied using a fluorescence FAM-ODN instead of G3139. Free FAM-ODN, nontargeted FAM-ODN encapsulated lipoplex nanoparticles and Tf-targeted FAM-ODN encapsulated lipoplex nanoparticles were used in the transfection procedure described above. 1, 24, and 48 h post transfection the cells were washed twice with 1X PBS and analyzed by flow cytometry on a Beckman Coulter EPICS XL (Beckman Coulter) to investigate overall cellular interaction. A minimum of 10,000 events were collected under the LIST mode for each assay. The data was analyzed using WinMDI software.

Cellular binding and uptake of the lipoplex nanoparticles in K562 cells were also examined by laser scanning confocal microscopy. 48 h post transfection, cells were washed twice with 1X PBS followed by fixation with 2% paraformaldehyde for 30 min. Nuclei were stained with 20 μM of DRAQ5 (Biostatus Limited, Leicestershire, U.K.) for 5 min at room temperature. The cells were mounted on a poly-D-lysine coated cover glass slide (Sigma-Aldrich, St. Louis, MO). Green fluorescence of FAM-ODN and blue fluorescence of DRAQ5 were analyzed, and merged images were produced using Zeiss 510 META Laser Scanning Confocal Imaging Systems and LSM Image software (Carl Zeiss MicroImaging, Inc., NY).

3. Results and Discussion

3.1. Size Distribution and Zeta Potential of G3139 Encapsulated Lipoplex Nanoparticles. Lipoplex nanoparticles were prepared by coaxial electrospraying G3139 solution and lipid mixtures. The breakup of coaxial jets is not as well understood as that of single jets, although progress is being made,[33−35] and, thus, four factors were investigated for their effects on the sizes of lipoplex nanoparticles: G3139 concentrations (C_{G3139}: 0.5 mg/mL and 1 mg/mL), lipid concentrations (C_{lipid}: 10 mg/mL and 15 mg/mL), flow rates of G3139 solution (Q_{G3139}: 0.4 mL/h, 0.8 mL/h and 1.2 mL/h) and flow rates of lipids mixture (Q_{lipid}: 0.4 mL/h, 0.8 mL/h and 1.2 mL/h). In total 36 screening experiments were performed to investigate all possible combinations of the four factors, and Figure 2 shows the volume mean diameter of the lipoplex nanoparticles prepared under different conditions. Overall, particle sizes range from 100 to 2500 nm, and the flow rates of both the G3139 solution and the lipids mixture affect the size. When the flow rates of G3139 are lower than or equal to the flow rates of the lipid mixture, the size of the lipoplex nanoparticles is smaller, 100 to 200 nm. When the flow rates of G3139 are higher than the flow rates of the lipid mixture, the size of the lipoplex nanoparticles varies from 500 nm to 2500 nm.

Varying the flow rates and solution concentrations also changed the overall lipid/G3139 ratio. Figure 3 summarizes the particle size as well as the zeta potential measurements in terms of this parameter, and each symbol represents a distinct set of operating parameters. At low lipid/G3139 ratios the particles were large and the zeta potentials could be as low as −16 mV, suggesting that aggregates formed with the negatively charged G3139. When the lipid/G3139 ratio was high, the particle size approached 100 nm and the zeta potential was +20 mV. These particles are stabilized both by the positively charged lipids and by the DSPE-PEG. Finally, these results show that even when the lipoplex nanoparticles were prepared at the same lipid/G3139 ratio, their sizes and zeta potentials could vary significantly as the preparation conditions, i.e. as the actual flow rates and solution concentrations were changed. Careful control of the operating parameters can, however, produce lipoplex nanoparticles with appropriate sizes and stability. Our results are

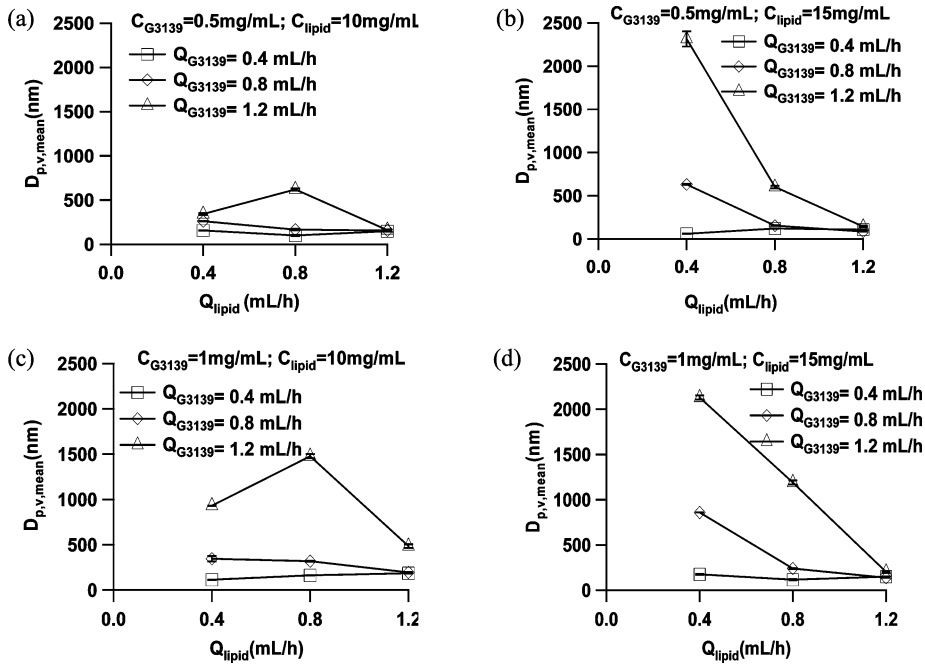

Figure 2. Effects of production parameters on the size $D_{p,v,\mathrm{mean}}$ of the lipoplex nanoparticles. Lipoplex nanoparticles were prepared at (a) G3139 concentration level of 0.5 mg/mL and lipid concentration level of 10 mg/mL, (b) G3139 concentration level of 0.5 mg/mL and lipid concentration level of 15 mg/mL, (c) G3139 concentration level of 1 mg/mL and lipid concentration level of 10 mg/mL and (d) G3139 concentration level of 1 mg/mL and lipid concentration level of 15 mg/mL. The flow rates of the G3139 solution (Q_{G3139}) and of the lipid mixture (Q_{lipid}) were 0.4, 0.8, and 1.2 mL/h. In these screening experiments only one sample was made for each operating condition. For each sample, $D_{p,v,\mathrm{mean}}$ was measured in triplicate.

consistent with the results of other coaxial jet studies that have shown that both particle size and structure can be functions of the flow rates of the inner and outer streams.[27,28,33−35] We plan to carry out more systematic studies to better understand the formation of lipoplex nanoparticles in the coaxial electrospray process.

Balancing the productivity, lipoplex nanoparticle size and zeta potential, the following production parameters were chosen to make G3139 encapsulated lipoplex nanoparticles for the rest of the study: the flow rates of the G3139 solution and the lipid mixture were both set at 1.2 mL/h, the concentration of the G3139 solution was 0.5 mg/mL and the concentration of the lipid mixture was 10 mg/mL. Under these conditions the final lipid/G3139 ratio was 20, the average particle size, based on 8 independently produced samples, was 190 ± 39 nm, and the zeta potential, based on 6 independently produced samples, was +4.5 ± 0.4 mV.

3.2. Structure of G3139 Encapsulated Lipoplex Nanoparticles. Small angle neutron scattering (SANS) and cryo-transmission electron microscopy (cryo-TEM) are complementary techniques used to characterize the structures of G3139 encapsulated lipoplex nanoparticles. Figure 4 illustrates typical SANS spectra for lipoplex nanoparticles made by electrospray under our standard conditions and by an ethanol dilution method. The latter sample is included to confirm that we can observe a Bragg peak in samples that have a periodic nanostructure, i.e. when the lipoplex nanoparticles are multilamellar. The SANS spectra for the lipoplex nanoparticles produced by electrospray never exhibited a Bragg peak even as the lipid/G3139 ratio varied from 10 to 20. In contrast, a Bragg peak was observed in the SANS spectrum of lipoplex nanoparticles prepared by ethanol dilution at a lipid/G3139 ratio of 12.5. From the position of the Bragg peak we can determine the interlamellar spacing d using the relation $d = 2\pi/q$, where $q = (4\pi/\lambda)\sin(\theta/2)$ is the momentum transfer vector. When we fit the peak for the lipoplex particles shown in Figure 4, using a Gaussian function, we found a center-to-center lamellar spacing of 6.6 ± 0.2 nm.

The cryo-TEM images support the SANS results by showing that most electrosprayed lipoplex nanoparticles have a unilamellar structure, while lipoplex nanoparticles prepared by ethanol dilution have onion-like multilamellar structure with center to center interlamella distance measured from the picture of about 7−10 nm. The difference in the structure of liposomes produced by coaxial electrospray and ethanol dilution may be due to the removal rate of ethanol from the solution. In electrospray, the liquids break into fine droplets, and the ethanol evaporates in less than 1 s due to the large surface area of the fine droplets (see Supporting Information). Thus, there may not be enough time available for the lipids and G3139 to form the multilamellar structure. In contrast, the ethanol dilution method uses dialysis to remove the ethanol, a process that usually takes about 24 h, and, therefore, there is enough time available to form the more complex multilamellar structure.

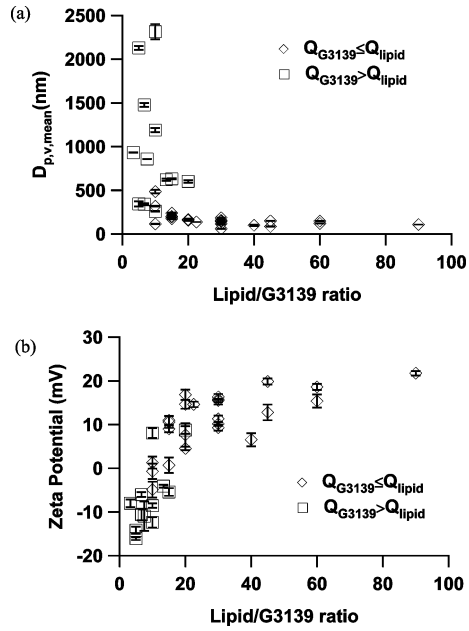

Figure 3. The effects of the lipid/G3139 ratio on (a) the size and (b) zeta potential of lipoplex nanoparticles prepared under the conditions shown in Figure 2. The lipid/G3139 ratio is calculated based on the flow rates and compositions of the inner and outer streams. We note that there is a one-to-one correspondence between the points in Figure 2 and Figure 3. Each symbol corresponds to a unique experiment (one of 36 operating conditions). The error bars are shown and are generally smaller than the symbol size. Different symbols are used to distinguish between experiments where $Q_{G3139} \leq Q_{lipid}$ and experiments where $Q_{G3139} > Q_{lipid}$.

3.3. G3139 Encapsulation Efficiency of Electrosprayed Lipoplex Nanoparticles. Gel electrophoresis was used to measure the G3139 encapsulation efficiency semiquantitatively. 1% Triton X-100 was used to break the lipid bilayers and release the encapsulated G3139. Free G3139 was loaded at concentration levels of 0.25, 0.5, 0.75, and 1 mg/mL to generate the standard curve. G3139 encapsulated lipoplex nanoparticles and the G3139 encapsulated lipoplex nanoparticles mixed with 1% Triton X-100 were loaded at concentration levels of 0.3 mg/mL. Figure 5 shows that without the treatment of 1% Triton X-100, no visible band was observed, suggesting that G3139 was encapsulated inside the lipoplex nanoparticles. With the treatment of 1% Triton X-100, a clear band formed in the gel, suggesting that G3139 was released from the lipid bilayers. Compared with the free G3139 standard curve, available in the Supporting Information, the encapsulation efficiency of G3139 in the electrosprayed lipoplex nanoparticles was 90 ± 6%.

3.4. Bcl-2 Downregulation. Chiu et al.[9] found that transferrin (Tf) conjugated lipoplex nanoparticles had targeting ability by binding to transferrin receptor (TfR), a transmembrane glycoprotein overexpressed on cancer and leukemia cells, and thus provided better downregulation of bcl-2 in K562 cells and was more effective for in vivo applications.[9] In this work the delivery efficiencies of both

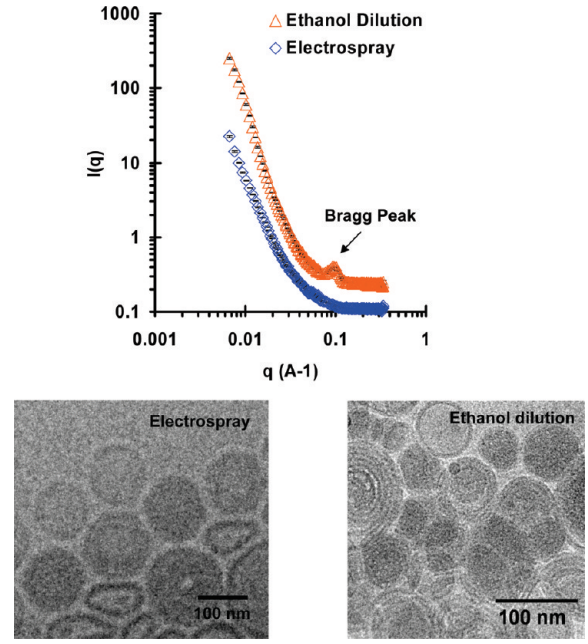

Figure 4. Typical SANS spectra and cryo-TEM images show that the electrosprayed lipoplex nanoparticles have unilamellar structure, while those prepared by ethanol dilution have a multilamellar structure. The error bars on the SANS data represent ±one standard deviation and are generally smaller than the symbol size. The electrosprayed lipoplex nanoparticles were prepared using our standard conditions: G3139 flow rate of 1.2 mL/h and concentration of 0.5 mg/mL, and the lipid mixture flow rate of 1.2 mL/h and concentration of 10 mg/mL.

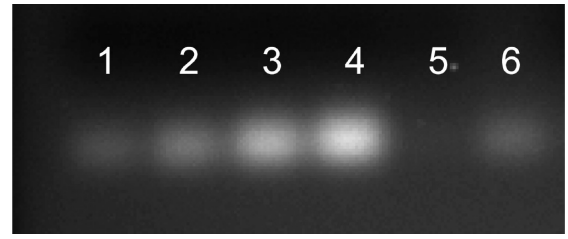

Figure 5. Gel electrophoresis shows that the encapsulation efficiency of electrosprayed lipoplex nanoparticles is very high. Lanes 1−4 are free G3139 standards at concentration levels of 0.25, 0.5, 0.75, and 1 mg/mL. Lane 5 contains the original G3139-encapsulated lipoplex nanoparticles. Lane 6 contains the G3139-encapsulated lipoplex nanoparticles that were treated with 1% Triton X-100. Lipoplex nanoparticles were prepared using a G3139 flow rate of 1.2 mL/h and concentration of 0.5 mg/mL, and a lipid mixture flow rate of 1.2 mL/h and concentration of 10 mg/mL.

nontargeted and Tf-targeted G3139 encapsulated lipoplex nanoparticles were evaluated based on the bcl-2 levels in K562 cells. Free G3139 was used as the control. The concentration of G3139 was set at 1 μM as suggested by Chiu et al.[9] 48 h post transfection the levels of bcl-2 were measured by Western blot. Figure 6 shows a representative Western blot result of bcl-2 protein expression. Densitometry analysis revealed that the bcl-2 levels were decreased by 57

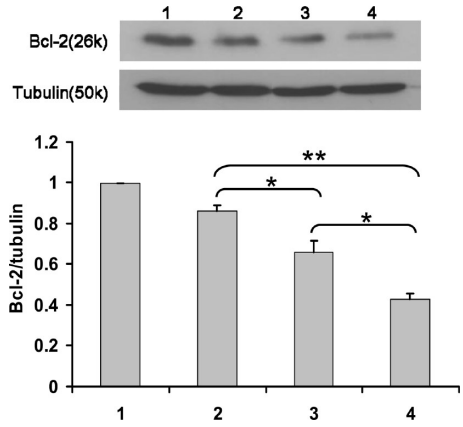

Figure 6. A representative Western blot of bcl-2 expression in K562 cells.1: Untreated cells. 2: Free G3139. 3: Nontargeted G3139 encapsulated lipoplex nanoparticles. 4: Tf-targeted G3139 encapsulated lipoplex nanoparticles. The concentration of G3139 was 1 μM. The Western blot was done 48 h post transfection. The lipoplex nanoparticles were prepared at a G3139 flow rate of 1.2 mL/h and concentration of 0.5 mg/mL, and a lipid mixture flow rate of 1.2 mL/h and concentration of 10 mg/mL. The error bars on the densitometry data are based on triplicate experiments made with independently produced batches of lipoplex nanoparticles. A Student *t*-test was used to determine which samples differed significantly at the $p < 0.05$ (*) and $p < 0.01$ (**) levels.

$\pm$ 3% when cells were transfected with G3139 in Tf-targeted lipoplex nanoparticles, compared to 34 $\pm$ 6% by G3139 in nontargeted lipoplex nanoparticles and 15 $\pm$ 4% by free G3139. The results were similar to those observed by Chiu et al.[9]

3.5. Cellular Uptake of ODN Encapsulated Lipoplex Nanoparticles. Flow cytometry was used to investigate the cellular uptake of FAM-ODN encapsulated lipoplex nanoparticles 1, 24, and 48 h post transfection. The conditions investigated included medium only (negative control), free FAM-ODN, nontargeted FAM-ODN encapsulated lipoplex nanoparticles and Tf-targeted FAM-ODN encapsulated lipoplex nanoparticles at a FAM-ODN concentration level of 1 μM (Figure 7). At all three time intervals the fluorescence signal of cells transfected with nontargeted FAM-ODN encapsulated lipoplex nanoparticles and Tf-targeted FAM-ODN encapsulated lipoplex nanoparticles was much higher than that of those transfected with free FAM-ODN: $\approx$10 times higher 1 h post transfection, $\approx$5 times higher 24 h post transfection and $\approx$4 times higher 48 h post transfection. We found that the advantage of FAM-ODN encapsulated in lipoplex nanoparticles as compared to free FAM-ODN decreased at later time points. This is because the cells continued to grow and the total cell number increased after 48 h, and, thus, the percentage of transfected cells over total cells decreased leading to the leveling off of the advantage of encapsulated FAM-ODN over free FAM-ODN. At 1 h post transfection there was no significant difference between the nontargeted FAM-ODN encapsulated lipoplex nanoparticles and Tf-targeted FAM-ODN encapsulated lipoplex

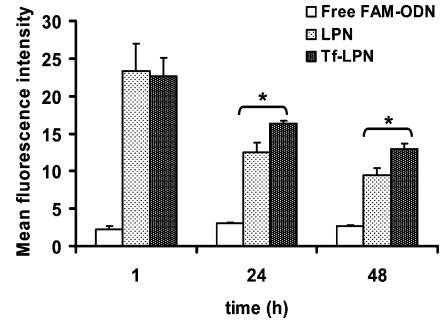

Figure 7. Flow cytometry. K562 cells were transfected with free FAM-ODN, nontargeted FAM-ODN encapsulated lipoplex nanoparticles (LPN) and Tf-targeted FAM-ODN encapsulated lipoplex nanoparticles (Tf-LPN). The FAM-ODN concentration was set at 1 μM. The lipoplex nanoparticles were prepared using an ODN flow rate of 1.2 mL/h and concentration of 0.5 mg/mL, and a lipid mixture flow rate of 1.2 mL/h and concentration of 10 mg/mL. The error bars correspond to triplicate experiments made with independently produced batches of lipoplex nanoparticles. A Student *t*-test was used to determine which samples differed significantly at the $p < 0.05$ (*) level.

nanoparticles; however, due to the targeting ability the latter had a higher fluorescence signal than the former at 24 and 48 h post transfection: $\approx$30% higher 24 h post transfection and $\approx$40% higher 48 h post transfection. In addition, confocal microscopy was used to demonstrate the internalization of the lipoplex nanoparticles. As shown in Figure 8, both nontargeted and Tf-targeted FAM-ODN encapsulated lipoplex nanoparticles were efficiently internalized by the cells and the level of cellular uptake was significantly higher than that of free FAM-ODN. The cellular uptake of nontargeted FAM-ODN encapsulated lipoplex nanoparticles was based on electrostatic interaction; however, for in vivo applications nontargeted lipoplex nanoparticles might be less effective due to nonspecific binding, rapid clearance by the reticuloendothelial system, or side effects, such as nonspecific cytokine production.[9]

4. Conclusions

We developed a coaxial electrospray process to produce ODN encapsulated lipoplex nanoparticles for gene delivery. The lipoplex nanoparticles produced by coaxial electrospray can be collected for intravenous injection, or transported via a sheath air flow for inhalation therapy. This method allows for better control over the way in which the lipids and aqueous phases are mixed. Compared with the standard ethanol dilution technique, coaxial electrospray is a simple one-step procedure that significantly reduces the time and effort required to produce the lipoplex nanoparticles and, furthermore, fairly monodisperse lipoplex nanoparticles can be produced. G3139 was successfully encapsulated in lipoplex nanoparticles via coaxial electrospray, and the size of the lipoplex nanoparticles was found to depend mainly on the flow rates and concentrations of the G3139 solution and the lipid

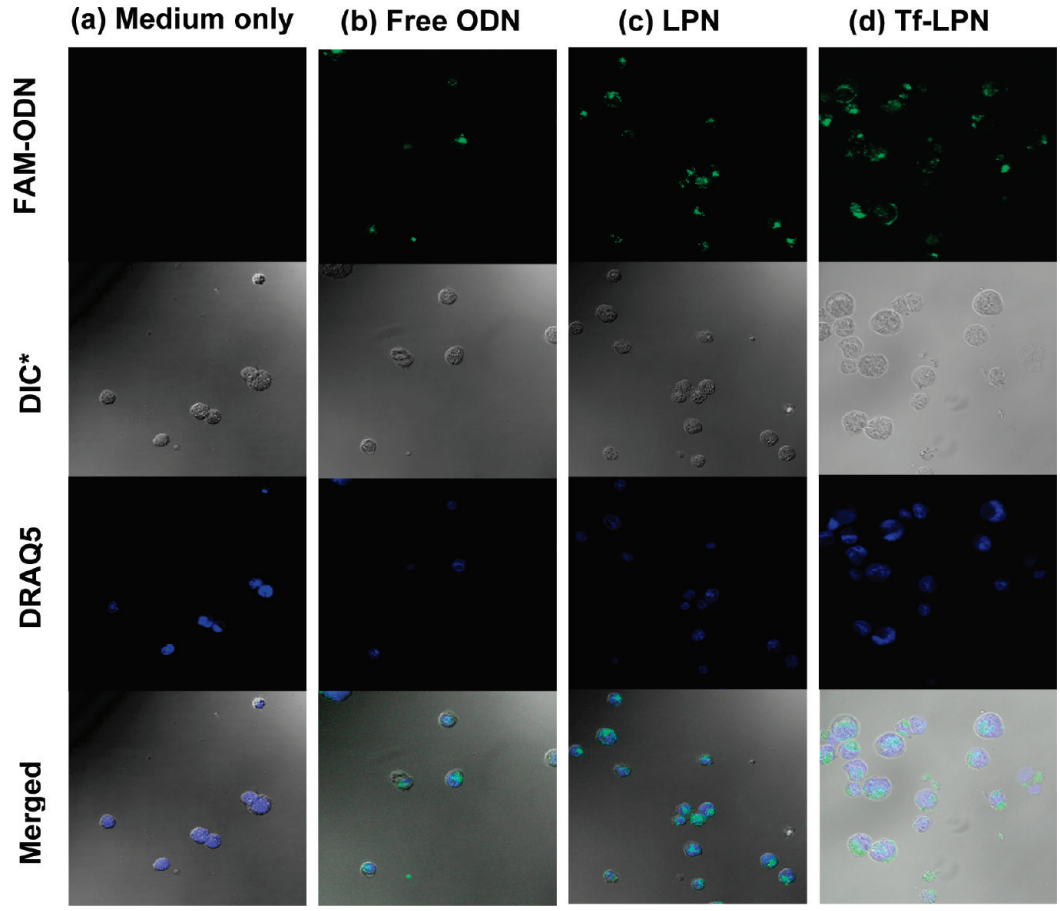

Figure 8. Confocal microscopy images show that green fluorescence of FAM-ODN and blue fluorescence of DRAQ5 (nucleus stain) colocalize inside K562 cells, suggesting that FAM-ODN is taken up by K562 cells. K562 cells were treated with (a) medium only (negative control), (b) free FAM-ODN, (c) nontargeted FAM-ODN encapsulated lipoplex nanoparticles (LPN) and (d) Tf-targeted FAM-ODN encapsulated lipoplex nanoparticles (Tf-LPN). The FAM-ODN concentration was set at 1 μM. The lipoplex nanoparticles were prepared using an ODN flow rate of 1.2 mL/h and concentration of 0.5 mg/mL, and a lipid mixture flow rate of 1.2 mL/h and concentration of 10 mg/mL. *DIC: differential interference contrast.

mixture. Lipoplex nanoparticles with diameter of 190 ± 39 nm, zeta potential of +4.5 ± 0.4 mV and G3139 encapsulation efficiency of 90 ± 6% were produced using a G3139 flow rate of 1.2 mL/h and concentration of 0.5 mg/mL, and a lipid mixture flow rate of 1.2 mL/h and concentration of 10 mg/mL. Unlike the ethanol dilution method, the lipoplex nanoparticles produced by coaxial electrospray with lipid/ODN ratio varied in the range of 10 to 20 all possess unilamellar structure. Transferrin was successfully conjugated to the electrosprayed lipoplex nanoparticles and provided targeting ability for the leukemia cellular uptake. G3139 in both nontargeted and Tf-targeted lipoplex nanoparticles was efficiently delivered to K562 cells and downregulated the bcl-2 protein expression by 34 ± 6% and 57 ± 3% respectively.

Supporting Information Available: Additional information as noted in text. This material is available free of charge via the Internet at http://pubs.acs.org.

MP9000348